Comparison of Two Reliability Assessment Methods for the Seismic Performance of Timber-Steel Hybrid Structures

Frank Lam
Professor, Dept. of Wood Science, University of British Columbia, Vancouver, Canada

Zheng Li
Assistant Professor, Dept. of Structural Engineering, Tongji University, Shanghai, China

Minjuan He
Professor, Dept. of Structural Engineering, Tongji University, Shanghai, China

Minghao Li
Lecturer, Dept. of Civil & Natural Resources Engineering, University of Canterbury, Christchurch, New Zealand (formerly Post-doctoral fellow, University of British Columbia, Vancouver, Canada)

ABSTRACT: The seismic performance of a multistory timber-steel hybrid building system with steel moment resisting frame, timber-steel hybrid diaphragms, and in-fill light frame wood shear walls has been studied. This paper focuses on the seismic reliability of the lateral load resisting system in such hybrid structures. The seismic performance of such hybrid systems has been evaluated using two reliability assessment methods with the consideration of the uncertainties from ground motion, intensity measure and structural resistance. One method was the fragility analysis which calculates the exceeding probability of drift demand from conditional distributions under given seismic intensity levels. Combined with a seismic hazard analysis, the failure probabilities for the timber-steel hybrid systems were obtained. The other method was response surface method (RSM), and polynomial functions were used to represent the seismic response surfaces. Non-performance probabilities were then evaluated by FORM with respect to different performance targets. Results from the two methods were compared showing similar results. However, the reliability indices obtained from RSM were lower than those obtained from fragility analysis. This was mainly due to the additional uncertainties considered in RSM. The associated reliability indices and failure probabilities for the timber-steel hybrid structures were also presented. Both methods may serve as tools for the reliability assessment of timer-steel hybrid structural systems, which supports more of its practical applications.

Severe structural damage and even collapse of buildings have been observed in recent major earthquakes around the world. The post-earthquake survey revealed that the casualties were mainly caused by the collapse of masonry or concrete buildings with large seismic mass and poor construction quality. However, experiences from past major earthquakes showed that timber buildings, with light self-weight, performed relatively well to protect life safety. In order to provide an alternative for multi-story building systems in seismic prone zones, He et al. (2014) proposed a kind of timber-steel hybrid structure. The timber-steel hybrid structure is composed of steel moment-resisting frames and timber-steel hybrid diaphragms. Light wood frame shear walls are integrated into the steel moment-resisting frames, forming a hybrid shear wall to serve as the lateral load resisting system for the structure. The timber-steel hybrid diaphragm is composed of C-shaped steel joists and dimension lumber decking, and 30 mm thick cement mortar was casted on its top to improve serviceability performance. The self-weight of

the hybrid structure is largely reduced due to the application of wood elements. Moreover, in the timber-steel hybrid buildings, most of the structural members are pre-fabricated, which can ensure the construction quality. Experimental studies also revealed that the infill wood shear walls were very effective in resisting lateral loads together with the steel moment frame (He et al. 2014).

The engineering community has increasingly become convinced that the seismic performance of a building system should be evaluated more efficiently using probabilistic tools with reasonable performance-related criteria. The seismic performance for other multi-story timber / timber-hybrid building systems has attracted much research attention in the past decade (Buchanan et al. 2008; Ceccotti 2008; Fragiacomo et al. 2011; van de Lindt et al. 2010; Ceccotti et al. 2013). However, no research has been reported on studying the seismic performance of timber-steel hybrid structural systems using reliability-based approaches.

In this paper, the seismic reliability of timber-steel hybrid shear walls was evaluated by two approaches (fragility method; and response surface method with first order reliability method FORM). A verified numerical model was used to create a seismic response database for the hybrid wall systems with different structural configurations. Their reliability indices and failure probabilities were obtained and compared using the two approaches.

1. NUMERICAL MODEL

The structural configuration of the baseline timber-steel hybrid shear wall is shown in Figure 1. Mild carbon steel with a yielding strength of 235 MPa are used for the steel frame. The cross sections of H-150×100×6×9 and H-150×150×7×10 are used for beams and columns, respectively. For the infill wood shear wall, No. 2 and better grade Spruce-Pine-Fir (SPF) 38 × 140 mm dimension lumber with a spacing of 400 mm is used as framing members, and 15mm-thick OSB panels are used as the sheathing material. The top plate and side studs of the infill wall are connected by bolted connections to the steel frame. The bolts transfer the shear force between the steel fame and the wood infill wall, and ensure that the infill wall and the steel frame could resist lateral loads together.

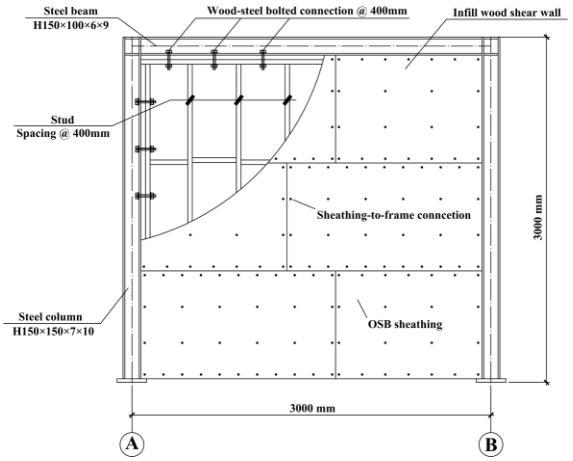

Figure 1: Configuration of baseline timber-steel hybrid shear wall.

The lateral stiffness ratio K_r for the infilled frame system can be defined as the ratio of the elastic stiffness between the infill wall and the steel frame, as shown in Eq. (1):

$$K_r = k_{\text{infill}} / k_{\text{bf}} \tag{1}$$

where $k_{\text{infill}} = 0.4P_{\text{infill}} / \Delta_{\text{infill}}$ and $k_{\text{bf}} = 0.4P_{\text{bf}} / \Delta_{\text{bf}}$, P_{infill} is the peak load resisted by the infill wood shear wall, kN; and Δ_{infill} is the lateral displacement of the infill wall at $0.4P_{\text{infill}}$, mm; P_{bf} is the peak load resisted by the bare steel frame, kN; and Δ_{bf} is the lateral displacement of the bare steel frame at $0.4P_{\text{bf}}$, mm.

In this study, the seismic performance of the hybrid shear walls with four K_r values (0.5, 1.0, 2.5 and 5.0) was evaluated. The different K_r values were achieved by designing the infill wood shear wall with different nailing schedules & panel thickness, as listed in Table 1. These numbers cover a range in practical applications of the timber-steel hybrid systems.

Table 1: Structural configurations of infill walls for different relative lateral infill-to-frame stiffness ratios.

Kr	*Nail type*	*Sheathing*	*Sheathing pattern*
0.5	*CN50*[a]	*9.5mm OSB*	*One side*
1.0	*CN50*	*9.5mm OSB*	*Both sides*
2.5	*12d common nail*[b]	*14.7mm OSB*	*One side*
5.0	*12d common nail*	*14.7mm OSB*	*Both sides*

Note: [a] CN50 nail is confirmed to the Japanese Industrial Standards (JIS), with 50 mm in length and 2.87 mm in diameter.

[b] 12d common nail is confirmed to ASTM F1667-11a (Standard Specification for Driven Fasteners: Nails, Spikes, and Staples), with 82 mm in length and 3.8 mm in diameter.

A nonlinear finite element (FE) model was developed in ABAQUS software package to simulate the seismic response of the timber-steel hybrid shear walls. As a general FE software package, ABAQUS does not have appropriate hysteretic elements to fully consider the strength and stiffness degradation and pinching effects of nail connections or wood shear walls. Thus, a so called "pseudo nail" algorithm was implemented into ABAQUS by Li et al. (2014a) as a user-defined subroutine to represent the hysteretic behavior of the infill wood shear wall. The "pseudo nail" model was proposed by Gu and Lam (2004) to represent the load-drift hysteresis of a wood shear wall using a nailed connection model. Of course, the nailed connection model parameters need to be calibrated in order to match the magnitudes of actual shear wall forces and drifts. The "pseudo nail" wall model has been shown to be computationally efficient and capable of modeling the behavior of wood shear walls under both static and dynamic loads (Gu and Lam 2004; Li and Lam 2009; Li et al. 2009; Li et al. 2012). A pair of user defined "pseudo nail" spring elements was used to model the racking behavior of the infill wood wall in the hybrid shear wall system. The developed FE model for the timber-steel hybrid shear wall system in ABAQUS is shown in Figure 2. Detailed information for the numerical model and its verification can be found in Li et al. (2014a).

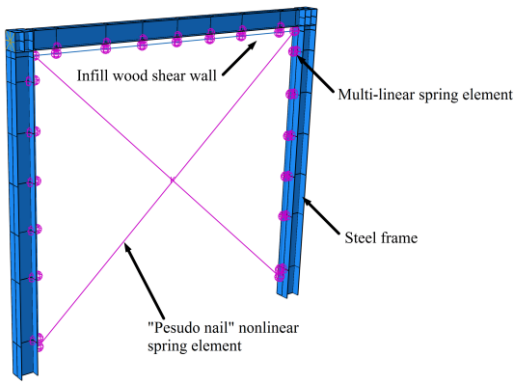

Figure 2: FE model for timber-steel hybrid shear wall system.

2. SEISMIC INPUT AND PERFORMANCE OBJECTIVES

In order to account for a seismic prone zone, several destructive records were selected in this study. Three performance level were considered according to Chinese Standard for Seismic Design of Building (CCSDB, 2011). The ground motion records used in this study are listed in Table 2.

CCSDB has defined immediate occupancy (IO), life safety (LS) and collapse prevention (CP) limit states, and the 50-year exceedance probabilities for the earthquakes considered in the IO, LS and CP limit states are 63%, 10% and 2%, in accordance with the average return period of 50, 475, and 2475 years, respectively. In this study, the spectral accelerations corresponding to these performance levels were 0.16, 0.45 and 0.90g, respectively. These ground motion records were then scaled to seismic hazard levels via a response spectrum approach, i.e., the 5% damped spectral value over the plateau region (0.1 - 0.65s) should match the design spectral value according to CCSDB.

In order to study the relationship between shear wall responses and seismic hazard levels, nonlinear time history analyses were performed at fifteen different spectral acceleration (Sa) levels (0.10, 0.16, 0.30, 0.45, 0.60, 0.75, 0.90, 1.05, 1.20, 1.35, 1.50, 1.65, 1.80, 2.05 and 2.10

g), and the ground motion records were scaled to these spectral acceleration values, respectively.

Table 2: Ground motion records used in analysis.

NO.	*Event*	*Date*	*Station*	*Component*	*PGA (g)*
1	*Wenchuan*	*12/05/2008*	*Wolong*	*EW*	*0.976*
2	*Tangshan*	*28/071976*	*Beijing Hotel*	*EW*	*0.067*
3	*Ninghe*	*25/11/1976*	*Tianjin Hospital*	*NS*	*0.149*
4	*Qian'an*	*31/08/1976*	*M0303 Qianan lanhe bridge*	*NS*	*0.135*
5	*Chichi*	*21/09/1999*	*CHY006*	*NS*	*0.345*
6		*21/09/1999*	*TCU070*	*EW*	*0.255*
7		*21/09/1999*	*TCU106*	*NS*	*0.128*
8		*21/09/1999*	*TAP052*	*NS*	*0.127*
9	*Kobe*	*17/01/1995*	*0 KJMA*	*KJM000*	*0.821*
10	*Northridge*	*17/01/1994*	*0013 Beverly Hills - 14145 Mulhol*	*MUL009*	*0.416*
11		*17/01/1994*	*24278 Castaic - Old Ridge Route*	*ORR090*	*0.568*
12		*17/01/1994*	*90086 Buena Park - La Palma*	*BPK090*	*0.139*
13	*Loma Prieta*	*18/10/1989*	*47381 Gilroy Array #3*	*G03000*	*0.555*
14		*18/10/1989*	*57425 Gilroy Array #7*	*GMR000*	*0.226*
15		*18/10/1989*	*58224 Oakland - Title & Trust*	*TIB180*	*0.195*

The performance requirements of a building system subjected to seismic loads can be defined by structural peak responses, e.g. maximum forces, stresses, or deformations. It is generally accepted in performance based seismic engineering that deformation limit states tend to a straightforward measure which is related to both structural and non-structural damage. According to a damage assessment process after the experiments, which had been presented in Li et al. (2014b), the drift ratios of 0.7%, 2.5% and 5.0% were considered as reasonable drift limits for the IO, LS and CP performance levels for the hybrid system, respectively. However, it should be noted that the drift limit for the CP performance level may still require some further discussions and verifications based on more full-scale experimental investigations in future studies.

3. FRAGILITY ANALYSIS

Seismic fragility $F_R(z)$ describes the conditional probability of reaching or exceeding a specified deterministic or random performance level with an intensity measure z, and it is defined as

$$F_R(z) = P[\theta_{max} \geq \theta_{PL} \mid S_a = z] \qquad (2)$$

where θ_{max} is the maximum inter-story drift from the analysis, θ_{PL} is the drift limit according to different performance levels. It is quite convenient to estimate probabilities of non-performance with the cumulative distribution functions (CDFs). Therefore, the fragility of a structural system is commonly expressed as a lognormal cumulative distribution function

$$F_R(z) = \Phi\left(\frac{In(z/m_R)}{\xi_R}\right) \qquad (3)$$

where $\Phi(\cdot)$ = standard normal cumulative distribution function; z is the given demand, which is spectral acceleration S_a; m_R is the median capacity; and ξ_R is the logarithmic standard deviation of capacity. Fragility curves can provide information on expected performance at given hazard levels in a concise manner and are easily interpreted by design engineers.

Figure 3 shows a set of sample peak displacement fragility curves for the hybrid shear walls with the lateral infill-to-frame stiffness ratio of 2.5 under different limit states.

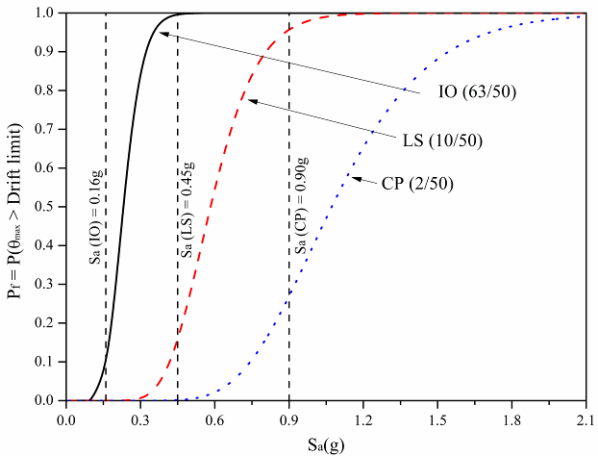

Figure 3: Peak displacement fragility curves of the hybrid shear wall with K_r = 2.5

For a structure or a structural assembly, the general formulation of the failure probability can be described as

$$P_f = \int P[G<0 \mid IM = z] f_{IM}(z)dz \qquad (4)$$

where $f_{IM}(z)$ is the probability density function of earthquakes with the intensity measure $z = S_a$. The discrete form of Eq. (4) can be expressed as

$$P_f = \sum P[G<0 \mid IM = S_a] P_{IM}(S_a) \qquad (5)$$

where $P_{IM}(S_a)$ is the annual probability of exceeding a given spectral acceleration S_a, and it can be estimated by a power law relationship as suggested by Cornell et. al. (2002)

$$P_{IM}(S_a) = k_s S_a^{-k_d} \qquad (6)$$

The IO, LS and CP hazard levels are in correspondence to the earthquake event with a mean return period of 50, 475, and 2,475 years, respectively. The annual spectral acceleration hazard curve $P_{IM}(z)$ was obtained by using Eq. (6) to fit to the S_a values with their corresponding return periods. The regression analysis yielded a value for the decay factor k_d of 2.25273, and a value of 0.00033 for the scale factor k_s. The failure probabilities for the timber-steel hybrid shear walls were then obtained by Eq. (5). Table 3 summarizes the annual failure probability estimates of exceeding the peak wall displacement limits and the corresponding reliability indices (β). It was also found that under the three performance levels, stronger infill wood shear wall was able to significantly reduce the failure probability of the hybrid shear wall system.

4. RESPONSE SURFACE METHOD

For response surface method, the performance function is described as Eq. (7):

$$G = \delta - \Delta(S_a, K_r, \varepsilon) \qquad (7)$$

where δ is the wall drift capacity, calculated as $\delta = H \cdot \theta_{PL}$; H is the wall height and θ_{PL} is the drift ratio limit corresponding to different performance objectives; Δ is the peak drift demand, which is a function of the seismic intensity measure S_a, lateral infill to frame stiffness ratio K_r and the response surface fitting error ε. The intensity measure of ground motions can be represented by the spectral accelerations S_a in accordance with the CCSDB. S_a is assumed to follow a lognormal distribution with mean of 0.115 g and coefficient of variation (COV) of 1.0, and the annual Poisson arrival rate of earthquake was assumed as 0.1/year. Over the suite of ground motions scaled to one spectral acceleration level and a given K_r, the mean ($\overline{\Delta}_{sm}$) and standard deviation ($\sigma_{\Delta sm}$) of the peak drifts responses were calculated. Therefore, for all the combinations of $\sigma_{\Delta sm}$ and S_a, a discrete set of $\overline{\Delta}_{sm}$ and a discrete set of $\sigma_{\Delta sm}$ can be obtained, respectively.

Table 3: Annual seismic failure probability and reliability indices obtained from fragility analysis.

Hybrid shear wall	*Immediate occupancy*		*Life safety*		*Collapse Prevention*	
	P_f	β	P_f	β	P_f	β
K_r=0.5	3.920×10^{-2}	1.760	4.405×10^{-3}	2.619	9.390×10^{-4}	3.109
K_r=1.0	2.298×10^{-2}	1.996	1.709×10^{-3}	2.927	4.441×10^{-4}	3.324
K_r=2.5	8.307×10^{-3}	2.395	9.174×10^{-4}	3.116	3.243×10^{-4}	3.410
K_r=5.0	6.865×10^{-3}	2.464	5.321×10^{-4}	3.273	2.278×10^{-4}	3.506

Then, polynomial functions, Eq. (8) were used to fit these peak drifts over the domain of random variables, respectively.

$$\begin{aligned}\overline{\Delta}_{rs} &= a_1 S_a K_r + a_2 S_a K_r^2 + a_3 S_a^2 K_r \\ &+ a_4 S_a^2 K_r^2 + a_5 S_a K_r^3 + a_6 S_a^3 K_r \\ &+ a_7 S_a^2 K_r^3 + a_8 S_a^3 K_r^2 + a_9 S_a^3 K_r^3\end{aligned} \tag{8a}$$

$$\begin{aligned}\sigma_{\Delta rs} &= b_1 S_a K_r + b_2 S_a K_r^2 + b_3 S_a^2 K_r \\ &+ b_4 S_a^2 K_r^2 + b_5 S_a K_r^3 + b_6 S_a^3 K_r \\ &+ b_7 S_a^2 K_r^3 + b_8 S_a^3 K_r^2 + b_9 S_a^3 K_r^3\end{aligned} \tag{8b}$$

where a and b are coefficients evaluated by minimizing the squared error between the polynomial fitting and the model simulation results. Now taking the RS fitting errors into account, the mean $\overline{\Delta}$ and standard deviation σ_Δ of the peak responses can be adjusted to

$$\overline{\Delta} = \overline{\Delta}_{rs}(1-\varepsilon_{\overline{\Delta}}) \tag{9a}$$

$$\sigma_\Delta = \sigma_{\Delta_{rs}}(1-\varepsilon_{\sigma_\Delta}) \tag{9b}$$

where $\varepsilon_{\overline{\Delta}}$ and $\varepsilon_{\sigma_\Delta}$ are random variables representing RS fitting errors and assumed to follow normal distributions. The mean and standard deviation of the overall fitting errors can be obtained when all combinations are considered. Using the assumption that peak drift responses follow a lognormal distribution, the performance function can be rewritten as Eq. (10).

$$G = \delta - \frac{\overline{\Delta}}{\sqrt{1+\nu_\Delta^2}} \exp(R_N \sqrt{ln(1+\nu_\Delta^2)}) \tag{10}$$

where $\overline{\Delta}$ is the mean of peak drift demand; ν_Δ is the coefficient of variation (COV); and R_N is the standard normal variate $R_N(0,1)$. Once the explicit performance function is obtained, and probability distributions for the random variables are given, the failure probability and reliability index β can be estimated by FORM.

Figure 4 shows the polynomial response surfaces with respect to S_a and K_r, as well as the fitted polynomial coefficients.

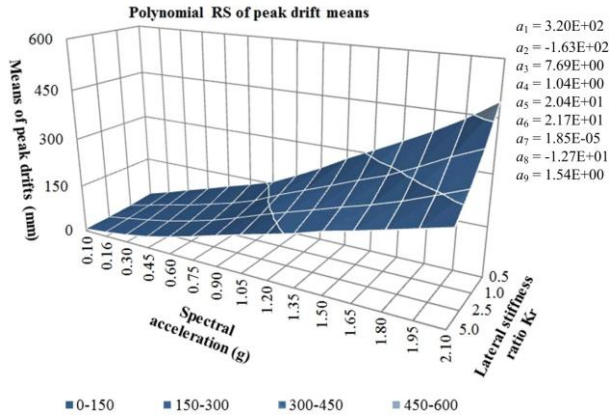

(a) Mean values

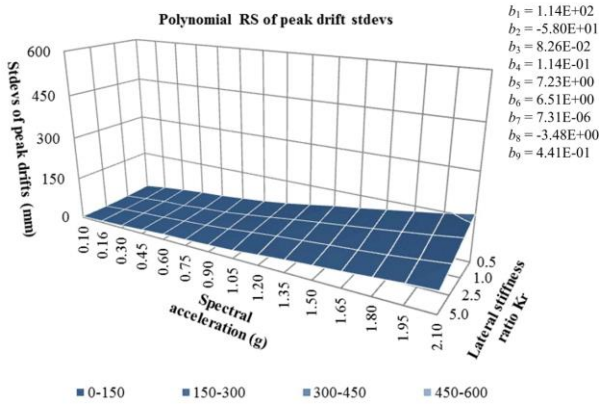

(b) Standard deviations

Figure 4. Simulation data and polynomial RS fitting parameters: (a) Mean values; (b) Standard deviations.

The software RELAN (Foschi et. al., 2007) was then used to calculate the failure probabilities. Table 5 gives the FORM results of the reliability indices with respect to different K_r values and performance levels. It is noted that under a given lateral stiffness ratio K_r, the β value of the IO performance level was between 1.832 and 2.438; for the LS performance level, the β value was between 2.560 and 3.224; and for the CP performance level, the β value was between 3.060 and 3.337. The reliability index increased about 0.73-0.82 for the LS limit state comparing with the IO limit state, and it increased by 0.15-0.50 for the CP limit state comparing with the LS limit state.

Table 4: Annual seismic failure probability and reliability indices obtained from FORM analysis.

Hybrid shear wall	*Immediate occupancy*		*Life safety*		*Collapse Prevention*	
	P_f	β	P_f	β	P_f	β
K_r=0.5	3.344×10^{-2}	1.832	5.237×10^{-3}	2.560	1.108×10^{-3}	3.060
K_r=1.0	2.071×10^{-2}	2.039	2.105×10^{-3}	2.862	5.026×10^{-4}	3.289
K_r=2.5	9.616×10^{-3}	2.341	1.069×10^{-3}	3.070	4.433×10^{-4}	3.324
K_r=5.0	7.381×10^{-3}	2.438	6.331×10^{-4}	3.224	3.663×10^{-4}	3.377

5. DISCUSSIONS AND CONCLUSIONS

The seismic reliability of timber-steel hybrid shear wall systems was evaluated using fragility analysis and response surface method. Results showed that although the failure probabilities calculated by the response surface method were slightly higher than those given by fragility analysis in some cases, the two methods gave very similar results. In the response surface method, a seismic response surface was firstly generated by dynamic analyses considering the intervening random variables and design parameters, and the response surface was fitted by polynomial functions. Thus, an explicit performance function was available for failure probability evaluations using FORM. Alternatively, other reliability methods (e.g. importance sampling, or Monte Carlo simulation) can also be used to calculate the failure probabilities. However, when the influence of one source of uncertainties (e.g., ground motions) is much larger than the other sources of uncertainties, fragility analysis appears to be a more straightforward way for the seismic analysis for a structural system. The fragility method is also very instructive for structural design purpose, and it is less complicated than a fully coupled reliability analysis since it separates the response analysis from the hazard analysis. In this study, it was found that both methods can be efficiently used in seismic reliability analysis for the hybrid shear wall systems. The results and reliability methods presented may be used for assessment purposes to evaluate vulnerability or expected damage or, when coupled with loss model, economic losses to timber-steel hybrid structures under seismic hazards.

6. ACKNOWLEDGEMENT

The authors would like to acknowledge the National Natural Science Foundation of China for supporting this work with a research grant (Grant No. 51378382).

7. REFERENCES

Buchanan, A. H., Deam, B., Fragiacomo, M., Pampanin, S., and Palermo, A. (2008). "Multi-storey prestressed timber buildings in New Zealand" *Structural Engineering International*, 18(2), 166-173.

Ceccotti, A. (2008). "New technologies for construction of medium-rise buildings in seismic regions: The XLAM case" *Structural Engineering International*, 18(2), 156-165.

Ceccotti, A., Sandhaas, C., Okabe, M., Yasumura, M., Minowa, C., and Kawai, N. (2013). "SOFIE project - 3D shaking table test on a seven-storey full-scale cross-laminated timber building" *Earthquake Engineering and Structural Dynamics*, 42(13), 2003-2021.

Chinese Standard GB 50011-2010 (CCSDB). (2010). "Chinese Code for Seismic Design of Buildings" National Standard of the People's Republic of China, Beijing, China. (in Chinese).

Cornell, C. A., Jalayer, F., Hamburger, R. O., and Foutch, D. A. (2002). "Probabilistic Basis for 2000 SAC Federal Emergency Management Agency Steel Moment Frame Guidelines" *Journal of Structural Engineering*, 128(4), 526-533.

Fragiacomo, M., Dujic, B., and Sustersic, I. (2011). "Elastic and ductile design of multi-storey cross-lam massive wooden buildings under seismic actions" *Engineering Structures*, 33(11), 3043-3053.

Foschi, R. O., Li, H., Folz, B., Yao, F., and Zhang, J. (2007). "RELAN - Reliability analysis software, V8.0" University of British Columbia, Vancouver, Canada.

Gu, J. and Lam, F. (2004). "Simplified mechanics-based wood frame shear wall model" *Proceedings of 13th World Conference on Earthquake Engineering*, Paper No. 3109. Vancouver, Canada.

He, M., Li, Z., Lam, F., Ma, R., and Ma, Z. (2014). "Experimental investigation on lateral performance of timber-steel hybrid shear wall systems" *Journal of Structural Engineering*, 140(4), 04014029-1-12.

Li, M., Foschi, R. O., and Lam, F. (2012). "Modeling hysteretic behavior of wood shear walls with a protocol independent nail connection algorithm" *Journal of Structural Engineering*, 138(1), 99-108.

Li, M. and Lam, F. (2009). "Lateral performance of non-symmetric diagonal-braced wood shear walls" *Journal of Structural Engineering*, 135(2), 178-186.

Li, M., Lam, F., and Foschi, R. O. (2009). "Seismic reliability analysis of diagonal-braced and structural-panel-sheathed wood shear walls" *Journal of Structural Engineering*, 135(5), 587-596.

Li, Z., He, M., Lam, F., Li, M., Ma, R., and Ma, Z. (2014a). "Finite element modelling and parametric analysis of timber-steel hybrid structures" *Structural design of tall and special buildings*, 23(14), 1045-1063.

Li, Z., He, M., Li, M., and Lam, F. (2014b). "Damage assessment and performance-based seismic design of timber-steel hybrid shear wall systems" *Earthquakes and Structures*, 7(1), 101-117.

van de Lindt, J. W., Pei, S., Pryor, S. E., Shimizu, H., and Isoda, H. (2010). "Experimental seismic response of a full-scale six-story light-frame wood building." *Journal of Structural Engineering*, 136(10), 1262-1272.